ISBN: 978-3-95450-191-5 doi:10.18429/JACoW-SRF2017-THPB004

Content from this work may be used under the terms of the CC BY 3.0 licence (© 2017). Any distribution of this work must maintain attribution to the author(s), title of the work, publisher, and DOI.

IMPACT OF DURATION OF LOW TEMPERATURE DOPING ON SUPERCONDUCTING CAVITY PERFORMANCE *

P. N. Koufalis†, F. Furuta, J. J. Kaufman, M. Liepe, Cornell University, Ithaca, NY, USA

Abstract

Low temperature treatments of superconducting cavities in a low pressure atmosphere of nitrogen have been shown to introduce a 'Q-rise' up to moderate surface fields and an overall increase in quality factor, Q_0. We present preliminary results of a systematic study of the effect of doping time on superconducting cavity performance. We show that the introduction of impurities to the RF penetration layer can improve cavity performance and investigate the relationship between electron mean free path and the temperature-dependent component of the surface resistance.

INTRODUCTION

Low temperature treatments of niobium in a low pressure atmosphere of nitrogen introduces interstitial impurities in the RF penetration layer resulting in an increase in the density of scattering sites and, therefore, in a reduction of the electron mean free path, ℓ [1]. This leads to the ubiquitous 'Q-rise' – an increase in cavity quality factor Q_0 with increasing accelerating gradient, E_{acc}, up to moderate fields – and overall higher Q_0 values with respect to 'clean' niobium cavities. Varying the doping time and temperature during the low temperature treatment leads to different impurity concentrations in the RF penetration layer ($\sim 2\lambda_L$) and, thus, results in a different ℓ, allowing one to control the strength of the 'Q-rise' of the cavity [1].

We heat treated two 1.3 GHz TESLA-shaped [2] cavities with different doping durations and vertically RF tested them to obtain measurements of Q_0 as a function of E_{acc} at various T, surface resistance, R_S, vs. T at low fields (~4.5 MV/m), and resonance frequency, f_0, vs. T near T_c. We then used these RF measurements to compare cavity performance and extract relevant material properties such as residual resistance, R_0, the energy gap, $\Delta(0)/k_B T_c$, and the mean free path, ℓ. Additionally, we investigated the field dependence of R_0 and the temperature-dependent component of the surface resistance, R_{BCS}.

SURFACE TREATMENTS

Two 1.3 GHz TESLA-shaped niobium cavities were treated in a low temperature, low pressure atmosphere of continuously flowing nitrogen with different vacuum annealing times. One was a single-cell cavity, C4(P2), and the other a 9-cell cavity, MHI-02. A 'clean' single-cell niobium cavity, C1(P1), was prepared and tested to provide a baseline for cavity performance. Finally, a single-cell cavity, C4(P1), received a high-temperature nitrogen-doping (i.e. 800 °C) to compare the low temperature and high temperature treatments. The details of the cavity surface treatments are outlined in Table 1 and the bake profile for C4(P2) is shown in Fig. 1.

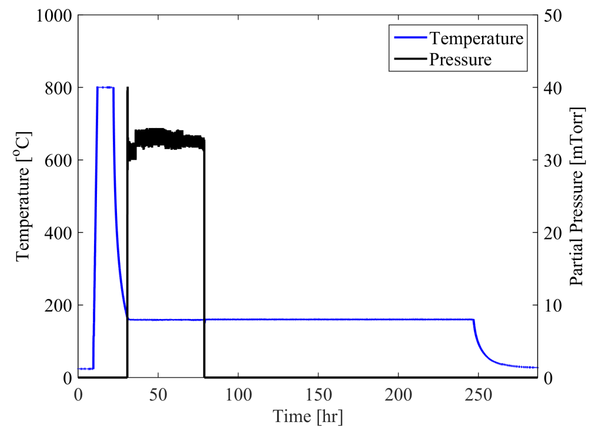

Figure 1: Temperature and nitrogen partial pressure profile for the heat treatment of cavity C4(P2).

The nitrogen atmosphere used during the doping step of C4(P2) and MHI-02 was continuously flowing as to constantly replenish trace impurities in the gas. The nitrogen used had 5 ppm O_2, 3 ppm H_2O, and 1 ppm of CO and CO_2. The heat treatments were completed sequentially in the order: de-gas, dope, and anneal. The cavities were not removed from the furnace in between each step.

Prior to heat treatment each cavity received a vertical electro-polish (EP) to remove inclusions, defects, and surface roughness and an ultra-sonic methanol rinse. Prior to assembly the cavities were cleaned with de-ionized water on a high pressure rinsing system to ensure a clean surface for RF testing. Cavity C4(P1) received a 24 μm vertical EP post-heat treatment to remove the lossy nitride layer that forms on the surface during the doping procedure [3,4].

RF PERFORMANCE

The low temperature doped cavities C4(P2) and MHI-02 both displayed the Q-rise and higher overall Q_0 values that is typical of high-temperature nitrogen-doped cavities [3,4]. In particular, the performance of C4(P2) was remarkably similar to that of C4(P1) reaching a maximum Q_0 of 3.6×10^{10} at E_{acc} = 16 MV/m – a factor of 1.6 increase over the Q_0 of the baseline cavity, C1(P1), at this field. The maximum field, E_{max} = 25 MV/m, reached by C4(P2) was limited by quench. Cavity MHI-02 reached a maximum Q_0 of 2.9×10^{10} at 14.6 MV/m and quenched at 23 MV/m. The

* Work supported by NSF Award PHYS-1416318.
† pnk9@cornell.edu

ISBN: 978-3-95450-191-5 doi:10.18429/JACoW-SRF2017-THPB004

Table 1: Cavity Surface Treatments

Cavity	De-gas	Dope	Anneal
C1(P1)	900 °C (3 hr; UHV)	–	–
C4(P1)	800 °C (3 hr; UHV)	800 °C (20 min; N_2)	800 °C (30 min; UHV)
C4(P2)	800 °C (10 hr; UHV)	160 °C (48 hr; N_2)	160 °C (168 hr; UHV)
MHI-02	800 °C (10 hr; UHV)	160 °C (48 hr; N_2)	160 °C (48 hr; UHV)

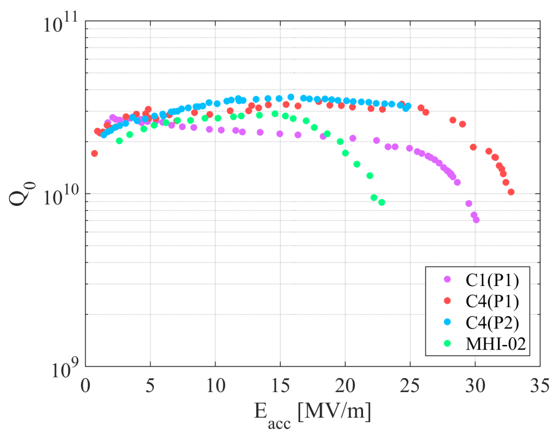

Figure 2: The RF performance at $T = 2.0$ K for the cavities listed in Table 1.

RF performance for each cavity test, in the form of Q_0 vs. E_{acc} measurements, is shown in Fig. 2.

The performance of the baseline cavity C1(P1) was quite typical for a cavity with a high temperature de-gas. The quality factor Q_0 decreased slowly from low to moderate fields (i.e. up to 25 MV/m), which is commonly referred to as medium-field Q-slope. The rapid decline of Q_0 at fields above 25 MV/m is the so-called high-field Q-slope. C1(P1) quenched at its maximum field of 30 MV/m and reached a Q_0 of 2.2×10^{10} at 16 MV/m. As is typical for such cavities, the maximum Q_0 was reached at very low fields (i.e. ~3 MV/m).

Decomposition of the surface resistance, R_S, into R_{BCS} and R_0 (see Fig. 3) revealed a field dependence of these components of cavities C4(P2) and MHI-02 very similar to that of the high-temperature nitrogen-doped cavity, C4(P1). This demonstrates that the reduction of R_{BCS} with increasing field is responsible for the observed Q-rise in all three doped cavities and the sharp increase in R_0 for cavity MHI-02 is responsible for the Q-slope observed near its quench field.

In clean niobium cavities (i.e. cavities with mean free path ranging from 200 to several thousand nm), R_{BCS} usually slightly increases with increasing field up to moderate fields [3–5]. The residual resistance R_0 is usually relatively constant from low to moderate fields but rapidly increases near the quench field resulting in the high-field Q-slope.

MATERIAL PROPERTIES

The SRIMP code [6, 7] was used to fit measurements of R_S vs. T at low fields and the penetration depth, λ, vs. T near the critical temperature, T_c, to extract the residual resistance R_0, energy gap $\Delta(0)/k_B T_c$, and mean free path ℓ of the four cavities listed in Table 1. The RF measurements of λ vs. T and corresponding BCS fits and material properties for C4(P2) are shown in Fig 4. The measurements of the surface resistance are used to extract the energy gap and residual resistance while the penetration depth data are used to extract the mean free path. Table 2 summarizes these material properties for each cavity.

Table 2: Cavity Material Properties Extracted from SRIMP

Cavity	$\Delta(0)/k_B T_c$	R_0 [nΩ]	ℓ [nm]
C1(P1)	1.82 ± 0.03	1.1 ± 0.3	–
C4(P1)	1.89 ± 0.03	1.8 ± 0.4	47 ± 14
C4(P2)	1.91 ± 0.03	2.8 ± 0.7	7 ± 1
MHI-02	2.18 ± 0.04	5.2 ± 1.2	0.8 ± 0.3

It is important to note that the mean free path of C4(P2) and MHI-02 are both very short compared to typical high-temperature nitrogen-doped cavities where ℓ can range from a few up to ~100 nm and, therefore, are considered heavily doped [4].

Cavity MHI-02 had a shorter mean free path with respect to C4(P2). The characteristic diffusion length, L, varies with $\sqrt{t}$ and, therefore, shorter anneal times result in shorter diffusion lengths. During the vacuum bake of MHI-02 and C4(P2) it is assumed that the total amount of impurities throughout the niobium remains constant. Thus, the shorter anneal time of MHI-02 resulted in higher impurity concentrations near the surface and hence a shorter mean free path.

SAMPLE ANALYSIS

Secondary ion mass spectroscopy (SIMS) analysis of a sample (see Fig. 5) baked alongside C4(P2) revealed high concentrations of C and O in the the RF penetration layer and relatively low concentration of nitrogen. The abundance of N throughout the RF layer was approximately two orders of magnitude smaller than that for C and O.

For comparison, we used SIMS to analyze a single crystal niobium sample that received a heavy 150 µm EP and an 800 °C deg-gas in ultra-high vacuum for 5 hrs. At this temperature, C, N, and O diffuse easily into the niobium bulk in the span of minutes. Therefore, the concentrations for these three impurities drops off quickly to background levels within the first 10 to 15 nm as can be seen in Fig. 5. The difference in nitrogen content between the de-gassed sample

Content from this work may be used under the terms of the CC BY 3.0 licence (© 2017). Any distribution of this work must maintain attribution to the author(s), title of the work, publisher, and DOI.

ISBN: 978-3-95450-191-5 doi:10.18429/JACoW-SRF2017-THPB004

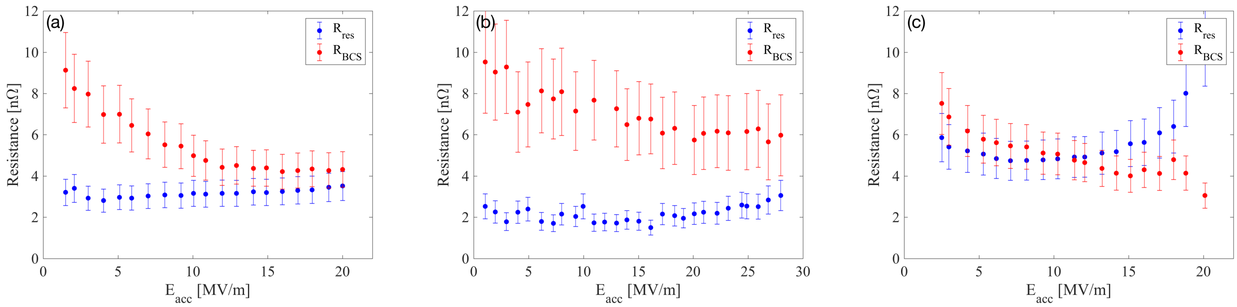

Figure 3: Field dependence of the temperature-dependent R_{BCS} and independent R_0 for **(a)** C4(P2), **(b)** C4(P1), and **(c)** MHI-02.

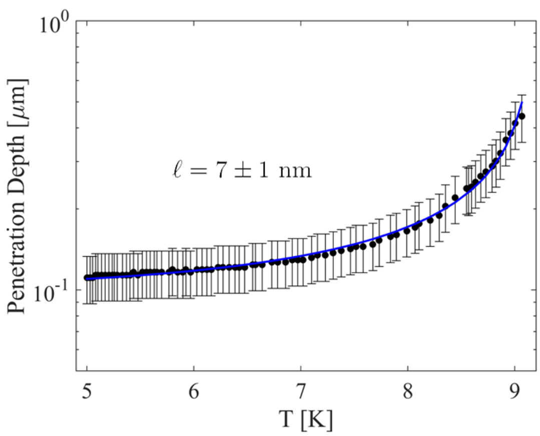

Figure 4: RF measurements of the penetration depth as a function of temperature and the corresponding BCS fit.

and the low temperature doped sample is very small; nitrogen should not diffuse more than a few nm at 160 °C [8, 9].

We estimated the mean free path using the measured concentrations of C and O at a depth of 50 nm in the low temperature doped sample; the relatively low concentration of N is insignificant. First the change in resistivity, $\Delta\rho$, was calculated using [5]:

$$\Delta\rho = a \cdot c' \tag{1}$$

where $a = 4.3 \times 10^{-8}$ Ω·m for C and 4.5×10^{-8} Ω·m for O and c' is the concentration of the impurity. At a depth of 50 nm, the concentration of C and O is 0.8 at. % resulting in $\Delta\rho_C = 3.4 \times 10^{-8}$ Ω·m and $\Delta\rho_O = 3.6 \times 10^{-8}$ Ω·m. The mean free path is then related to the change in resistivity by:

$$\ell = \frac{\sigma}{\Delta\rho_C + \Delta\rho_O} \tag{2}$$

where the constant $\sigma = 0.37 \times 10^{-15}\ \Omega \cdot \mathrm{m}^2$. Equation (2) yields a mean free path estimate of ~5 nm – in excellent agreement with the measure mean free path of 7 ± 1 nm. For more detailed calculations see Refs. [9, 10].

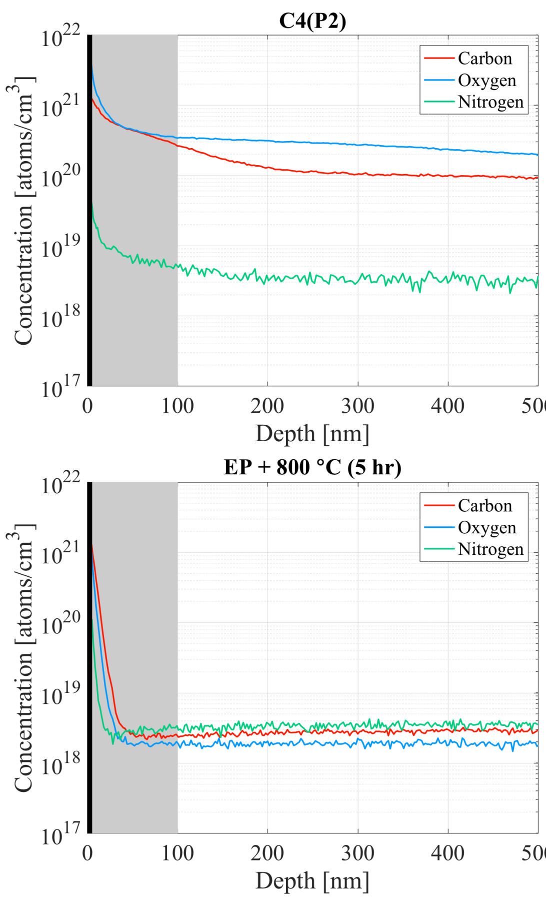

Figure 5: Secondary ion mass spectroscopy of a sample baked alongside cavity C4(P2) **(top)** and a single-crystal sample that received an 800 °C vacuum bake for 5 hr **(bottom)**. The black region represents the oxide layer (~5 nm) and the gray region represents the RF penetration layer (~100 nm $\approx 2\lambda_L$).

CONCLUSION

We presented preliminary results on the study of the impact of duration of low temperature doping on superconducting cavity performance and material properties. It was shown, that a shorter vacuum anneal time following the dop-

Content from this work may be used under the terms of the CC BY 3.0 licence (© 2017). Any distribution of this work must maintain attribution to the author(s), title of the work, publisher, and DOI.

ISBN: 978-3-95450-191-5 doi:10.18429/JACoW-SRF2017-THPB004

ing step results in high concentration of impurities near the surface resulting in shorter electron mean free path.

REFERENCES

[1] J. T. Maniscalco, M. Liepe, and D. Gonnella, "The Importance of the Electron Mean Free Path for Superconducting RF Cavities," *J. App. Phys.*, vol. 21, no. 043910, 2017.

[2] B. Aune *et al.*, "Superconducting TESLA cavities," *Phys. Rev. ST Accel. Beams*, vol. 3, no. 092001, 2000.

[3] A. Grassellino, A. Romanenko, D. Sergatskov, O. Melnychuk, Y. Trenikhina, A. Crawford, A. Rowe, M. Wong, T. Khabiboulline, and F. Barkov, "Nitrogen and argon doping of niobium for superconducting radio frequency cavities: a pathway to highly efficient accelerating structures," *Supercond. Sci. Tech.*, vol. 26, no. 102001, 2013.

[4] D. Gonnella, "The Fundamental Science of Nitrogen-Doping of Niobium Superconducting Cavities," Ph.D. dissertation, 2016.

[5] H. Padamsee, J. Knobloch, and T. Hays, *RF Superconductivity for Accelerators*, 2nd ed. Wiley, 2008.

[6] J. Halbritter, "FORTRAN-Program for the Computation of the Surface Impedance of Superconductors," Karlsruhe, Germany, Tech. Rep., 1970.

[7] N. Valles, "Pushing the Frontiers of Superconducting Radio Frequency Science: From the Temperature Dependence of the Superheating Field of Niobium to Higher-Order Mode Damping in Very High Quality Factor Accelerating Structues," Ph.D. dissertation, 2013.

[8] R. W. Powers and M. V. Doyle, "Diffusion of Intersitial Solutes in the Group V Transistion Metals," *J. Appl. Phys.*, vol. 30, no. 4, 1959.

[9] P. N. Koufalis, D. L. Hall, M. Liepe, and J. T. Maniscalco, "Effects of Intersitial Carbon and Oxygen on Niobium Superconducting Cavities," 2017, arXiv:1612.08291.

[10] P. N. Koufalis, J. T. Maniscalco, and M. Liepe, "Low Temperature Doping of Niobium Cavities: What is really going on?" 2017, presented at SRF2017, Lanzhou, China, paper TUXBA01, this conference.

Content from this work may be used under the terms of the CC BY 3.0 licence (© 2017). Any distribution of this work must maintain attribution to the author(s), title of the work, publisher, and DOI.